Journal of Alloys and Compounds 509 (2011) 6374–6381

Contents lists available at ScienceDirect

Journal of Alloys and Compounds

journal homepage: www.elsevier.com/locate/jallcom

Fabrication of crack-free blanket nanoporous gold thin films by galvanostatic dealloying

Oya Okman*, Jeffrey W. Kysar

Department of Mechanical Engineering, Columbia University, New York, USA

ARTICLE INFO

Article history:
Received 17 December 2010
Received in revised form 12 February 2011
Accepted 21 February 2011
Available online 1 March 2011

Keywords:
Nanoporous gold
Electrochemical dealloying
Galvanostatic
Potentiostatic
Thin film

ABSTRACT

A galvanostatic dealloying method, wherein the material removal rate is directly controlled, is proposed for fabrication of constrained crack-free nanoporous gold (NPG) films. Uniform, three-dimensional, crack-free, blanket NPG films are fabricated by this method from both low and high Au concentration precursor alloys up to 1300 nm thickness, which cannot be obtained by other methods. Ag dissolution rate proved to be critical in maintaining the film stress below the threshold value at which cracks develop. The findings contribute to understanding the formation mechanisms of NPG films.

1. Introduction

Nanoporous gold (NPG) is a bicontinuous network of ligaments and pores with sizes varying from 3 to 30 nm [1,2]. With a surface area to mass ratio from 10 m^2/g [3] to 150 m^2/g [4] and an excellent chemical stability, NPG films are promising candidates to serve as the functionalized layer of MEMS devices. Recent studies on the behavior of NPG upon electric charging of the surface show that NPG is an effective platform to convert capillary forces to macroscopic displacements leading to applications as sensors [5] and actuators [6–8]. A significantly higher density of atomic step edges on NPG compared to bulk gold makes NPG good catalysts for O_2 reduction in fuel cells [9] and in gas phase catalysis of methanol oxidation [10]. They are effective as biological platforms with respect to their low electrode–electrolyte impedance, which provides a superior signal to noise ratio for detection of neural activity [11]. In addition, the optical properties of NPG are significantly different than that of bulk gold. Since the pore size is usually much smaller than the wavelength of visible light, which is between 400 nm and 700 nm, significant surface plasmon resonance (SPR) can be achieved [12]. NPG is also a suitable material for tunable surface-enhanced Raman spectroscopy (SERS) [13,14]. Finally, methods to fabricate crack-free NPG have only been recently developed [15–18]. Most are intended for the fabrication of NPG in bulk form, although some are intended for NPG thin films deposited onto silicon substrates. It is clear that robust fabrication techniques of NPG in thin film form on substrates are necessary if NPG is to fulfill its promise in its diverse application areas, especially in micro-electro-mechanical systems (MEMS).

In principle, NPG films are fabricated by selective dissolution of the less noble element in a binary solid solution alloy, typically an Au–Ag alloy, that has complete solid solubility of the two elements. Selective removal of the Ag atoms is realized either by free corrosion [19] or by dealloying with an electrochemical cell [20]. Both methods provide crack-free NPG materials from precursor alloys in the form of unconstrained thin leafs [1,21] and millimeter scale ingots [22,23]. Senior and Newman [24] used a potentiostatic (i.e. potential-controlled) electrochemical dealloying method in an $HClO_4$ electrolyte and observed the occurrence of cracking on 100 μm thick Au–Ag sheets upon a step application of the potential. They reported improvements in NPG quality at higher temperatures and attributed it to enhanced surface diffusion of Au during dealloying. At lower potential values, they found the occurrence of cracking to be reduced and attributed the reduction to a lower Ag removal rate and a longer total dealloying time, which permits more time for Au surface diffusion to occur. A multi-step dealloying process introduced by Sun et al. [15] limits volume contraction and crack formation in bulk NPG. In addition, both potentiostatic and galvanostatic (i.e current-controlled) methods have been used to dealloy nickel-based superalloys in bulk form [25].

The dealloying of precursor alloy films constrained to a substrate has proven more challenging. Very thin (45–80 nm) alloy films deposited onto silicon substrates are successfully dealloyed

---

* Corresponding author at: 500 W. 120th St., Rm: 220, New York, NY 10027, USA. Tel.: +1 646 460 3966.
E-mail address: oo2128@columbia.edu (O. Okman).

0925-8388/$ – see front matter © 2011 Elsevier B.V. All rights reserved.
doi:10.1016/j.jallcom.2011.02.115

by free corrosion in concentrated nitric acid, which leads to crack-free blanket NPG films [14,16]. However, minor cracking is frequently reported during dealloying by free corrosion for thicker (250–400 nm) constrained precursor alloy films with compositions around 32 at.% Au [14]. Another method to fabricate crack-free NPG in free-standing beams is to induce thermal buckling prior to dealloying [26]. Finally, the occurrence of cracks in blanket NPG thin films of 250 nm thickness is significantly reduced with a potentiostatic method by application of the potential as a ramp function rather than a step function [17,18] using a three-electrode electrochemical cell.

Thus it has been shown that the propensity for cracking in NPG thin films is controlled by the competition between the rate of stress increase due to removal of the Ag atoms and the rate of stress relief from surface diffusion of Au. In free corrosion and in potentiostatic electrochemical dealloying, the rate of Ag removal is not controlled directly and varies significantly during the process. For the potentiostatic method, the rate of Ag removal reaches a maximum value after a critical potential value is exceeded and then decreases rapidly throughout the remainder of the dealloying process, irrespective of whether the potential is applied as a step or as a ramp [18]. The elevated Ag removal rate increases the risk of cracking.

In this study, a galvanostatic dealloying method using a three-electrode electrochemical cell is presented, in which the areal current density—and hence the Ag removal rate—is precisely controlled throughout the course of dealloying. Crack-free, blanket, NPG thin films are fabricated using this method that are significantly thicker than can be obtained by either free corrosion or by potentiostatic methods.

2. Experiment

Prior to deposition of the precursor alloy film, the silicon substrates are cleaned in acetone (Phramco-Aaper) in a sonicator for 5 min, then rinsed with isopropanol (99.8% pure Pharmco-Aaper), and finally baked at 150 °C on a hot plate for 10 min. Adhesion layers of 7 nm Cr and 30 nm Au are deposited by sputtering, at a base pressure of 2×10^{-6} Torr of Ar, in a vacuum deposition system (Kurt J. Lesker PVD 75).

Precise measurement of the areal current density during dealloying is critical in this study; thus the test specimens are designed to incorporate a precisely dimensioned area of the precursor Au/Ag alloy on the underlying Au film, Cr film and wafer. The Au layer serves two purposes: as a barrier to isolate the underlying Cr film from the electrolyte to prevent delamination; and, as a conductive layer to transmit current to the alloy during electrochemical dealloying. The regions of the Au/Ag precursor alloy are prepared using photolithography as demonstrated in Fig. 1. After deposition of the adhesion layers, the specimens are spin coated with LOR 3A (MicroChem Inc.) resist and then with Microposit S1813 (Shipley Company) photoresist. The LOR 3A is applied at different thicknesses ranging from 250 nm to 600 nm, depending on alloy film thickness; the photoresist layer is 1800 nm. The resist bilayer (cf. Fig. 1b) improves the integrity of the patterns during the lift off (cf. Fig. 1f). The samples are then exposed using either a Heidelberg μ PG 101 laser writer or a Süss MicroTec MJB3 Mask Aligner (cf. Fig. 1c). The sample pattern to be dealloyed is comprised of a rectangular region with an area that ranges from 6 mm^2 to 16 mm^2 along with a smaller area to be kept unexposed to the electrolyte in the further fabrication steps in order to preserve a sample of the original precursor alloy. The samples are then placed in the sputter deposition system and coated with the alloy of the desired composition using simultaneous sputter deposition of the Au and Ag. The grain size of the precursor alloy is about 40 nm for the 250 nm thick films and about 150 nm for the 1300 nm thick films. The resist is then removed using NANO™ Remover PG (MicroChem Corp.), leaving behind precisely patterned rectangular islands of Au/Ag alloy on an Au coated surface (cf. Fig. 1f). The photolithography methods used to pattern the surface provide dimensional accuracy of the order of micrometers.

The precursor Au/Ag alloy films are dealloyed using a three-electrode electrochemical cell, with a Pt counter electrode and an Ag/AgCl reference electrode (cf. Fig. 2). A potentiostat (μAutolab® Type III/FRA2) is used to control either the potential or the current. Herein, potentials are reported versus the reference electrode (0.200 V versus SHE). Aqueous perchloric acid (0.7 M) at 60 °C is used as the electrolyte. A 2 cm^2 platinum electrode mesh is used as the counter electrode, which is placed at a distance of 10 mm from the alloy film surface. Areal current density values are calculated based on the measured current history normalized by the projected area of the patterned Au/Ag island onto the substrate. Process parameters are chosen such that the potential remains below the oxidation potential of the Au so that Au is not removed from the film; thus essentially all current in the electrolyte can be attributed to Ag ions. After dealloying, the NPG films are cleaned with deionized water and blown dry by nitrogen. The films are imaged using a Hitachi 4700 Scanning Electron Microscope (SEM) at a working distance of around 8 mm, with an acceleration voltage of 10 kV and a beam current of 10 μA.

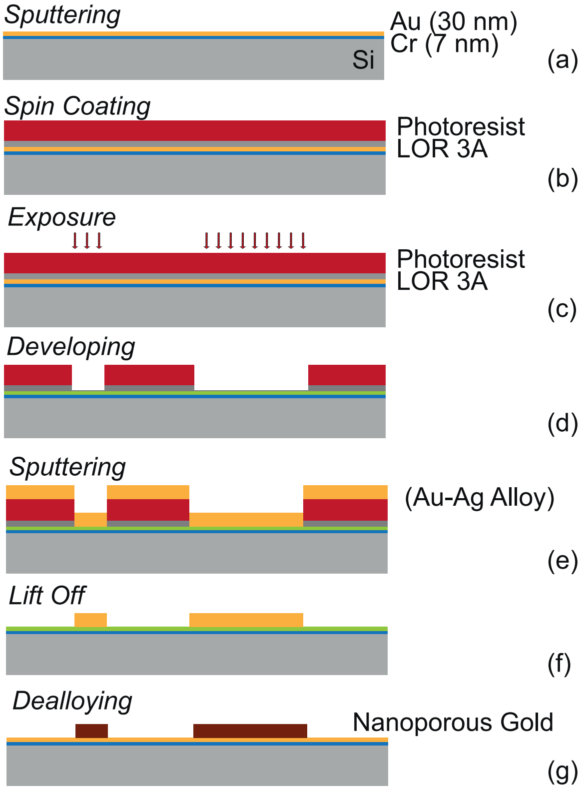

Fig. 1. Schematic representation of sample preparation: (a) sputtering of Cr and Au; (b) spin coating of the photoresist; (c) exposure through a photomask; (d) developing; (e) sputtering of Au–Ag alloy; (f) lift off; and, (g) dealloying.

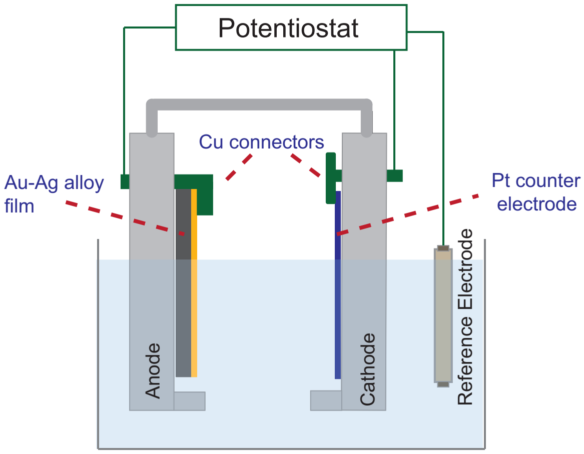

Fig. 2. Schematic representation of three-electrode electrochemical cell.

3. Background

The models in the literature [23,27,28] concerning dealloying mechanisms, the stress in NPG, as well as NPG shrinkage mainly address dealloying of unconstrained thin sheets and bulk metals that are relatively free to contract. Many of the dealloying procedures in the literature have a time scale of several hours (e.g. [23]), whereas in the present study the dealloying time is on the order of several seconds to a few minutes. Furthermore the grain sizes of some NPG in the literature (e.g. [23]) are many tens of micrometers whereas the grain size in the as-deposited films of the present study ranges from 40 nm to 150 nm. As a consequence, diffusion may play a much more important role in the present fabrication methods than in the other fabrication methods. Thus it is difficult to make a direct comparison of the present experimental results with existing models in the literature or with other fabrication procedures because of the high grain boundary surface area associated the much smaller grain size in the thin films of the present study as compared to grain sizes of precursor alloys of other studies.

During the dealloying process, Ag removal from the precursor alloy is accompanied by a significant shrinkage of up to 30% of the total volume if the material is unconstrained [23]. If the precursor alloy film is constrained to a substrate, it cannot reduce its in-plane dimensions significantly so an internal tensile stress is induced in the film [24]. On the other hand, the spinodal decomposition-based evolution of the nanoporous structure [29] involves diffusion of the Au on the film surface. In terms of the evolution of the film stress, the dealloying procedure involves two competing mechanisms: the rate of stress build-up due to removal of Ag from a precursor alloy constrained to a substrate and the rate of stress relief due to diffusion of the Au that could lead to a Coble creep type of mechanism. Thus, an effective way to prevent crack formation is to control the rate of Ag removal during dealloying so that the contribution of surface diffusion to stress relief can maintain the stress and hence, the strain energy density, below the threshold for fracture.

For a constrained precursor alloy, a tensile stress develops in the NPG film because the value of strain, $\varepsilon = \Delta L/L$, must remain very small. An upper bound for the mean biaxial stress, σ_m, in the NPG film is $\sigma_m \leq M_f \varepsilon_{unc}$, where M_f is the biaxial modulus of the NPG defined as $M_f = E_f/(1-\nu_f)$, and ε_{unc} is the strain in an unconstrained film; here E_f is Young's modulus and ν_f is Poisson's ratio of the NPG film. The high strain energy densities that would result from a ε_{unc} of 10% (that corresponds to a 30 vol% reduction) would certainly cause the film to fracture, especially since NPG is known to exhibit macroscopic brittleness [30,31]. The actual value of σ_m that develops in the constrained films upon dealloying is related to the $\Delta L/L$ that occurs during constrained dealloying, here called ε_{con}. Clearly then $\varepsilon_{con} = \sigma_m/M_f$. The value of σ_m can be as high as 90 MPa [16], which corresponds to a value of ε_{con} up to 0.008 based upon $E_f = 8.8$ GPa [32] and assuming a Poisson's ratio of $\nu_f = 0.2$ [21]. This is consistent with a residual stress of 65 MPa measured in Lee et al. [32].

In potentiostatic dealloying, the electric potential (i.e voltage) is controlled throughout the dealloying process and the electric current adopts a value determined by the potential and the electrochemical circuit [1,17,18,24]. The rate at which Ag is removed from the alloy film on the anode of the electrochemical cell is directly related to the electric current. A previous study on potentiostatic dealloying of NPG films [18] reported that for a potential of 1.2 V applied as a step function, the current density is initially as high as 400 mA/cm^2 and reduces to a value two orders of magnitude smaller as the dealloying continues. A qualitatively different current density history is seen if the potential is applied as a ramp rather than as a step. As the potential during the ramp exceeds the equilibrium potential, i.e. the open circuit potential of the cell, Ag atoms on the surface of the alloy film are dissolved in small amounts resulting in a small current density that increases with the applied potential. A peak in the Ag dissolution rate is observed when the potential exceeds the *critical potential*, η_c [33]. For the specific case in Okman et al. [18], the maximum current density during ramped application of the potential is about 14 mA/cm^2 (which occurs at a potential of about 1 V) and then reduces rapidly due to depletion of the Ag in the remaining precursor alloy to a value of about 2 mA/cm^2. Thus, the Ag dissolution rate is temporally highly nonuniform for both potential-controlled schemes. Nevertheless, for the same maximum potential value reached in the process, the ramped potential leads to a significantly lower maximum Ag dissolution rate than does the stepped potential scheme. Any increase in Ag dissolution rate is expected to be accompanied by a concomitant elevation of the stress level, so the ramped potential scheme is expected to yield better quality NPG thin films constrained to a substrate than the stepped potential scheme, as is borne out by the experimental results in Okman et al. [18].

4. Results

The main motivation for development of galvanostatic dealloying is to control the precise Ag dissolution rate throughout the dealloying process. With this method, the applied potential is regulated by a potentiostat to maintain a constant current density during dissolution of Ag from the precursor alloy and the attendant morphological changes that occur (cf. Fig. 3a). In this study, the current density is controlled to be a constant value between 1 and 10 mA/cm^2 throughout the dealloying process; an example of dealloying at a constant current density of 2.5 mA/cm^2 is shown in Fig. 3a for a precursor film of 30 at.% Au with initial thickness of 250 nm. The corresponding potential at any instant is a function

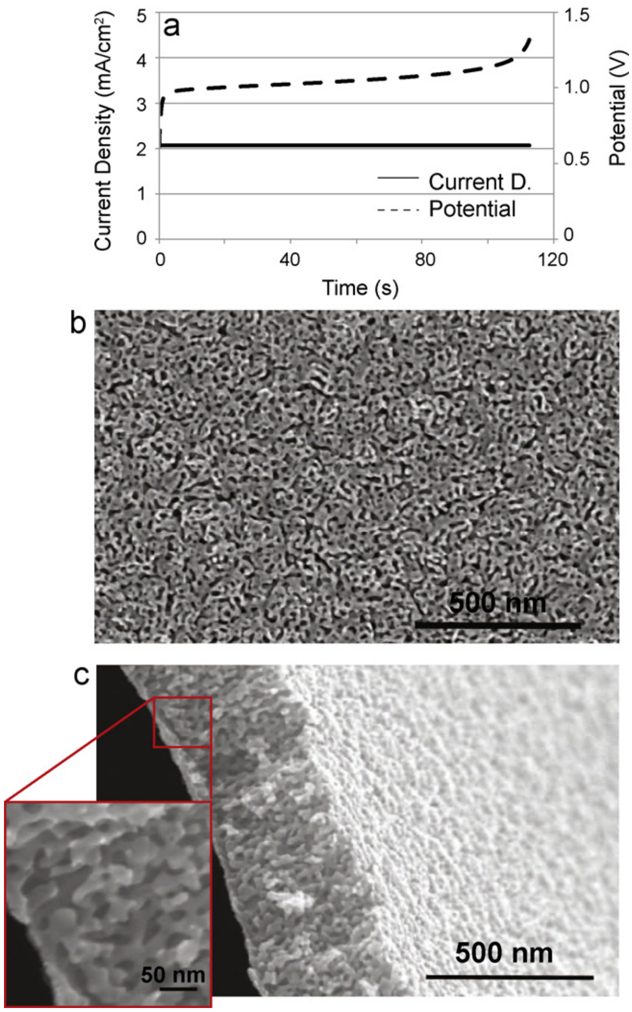

Fig. 3. NPG thin film fabricated from dealloying at constant current density of 2.5 mA/cm^2 from a precursor alloy film of 30 at.% Au: (a) variation of potential in galvanostatic dealloying; (b) surface of the NPG film; and, (c and inset) cross-section of NPG film.

of the morphology of the developing NPG structure as well as the residual Ag that remains in the film. Once the Ag concentration in the film nears depletion, the potential must increase to maintain a constant current density. The steep increase of the potential towards the end of the process in Fig. 3a indicates almost complete dissolution of Ag atoms in the alloy and therefore low residual Ag concentration in the final NPG film. If the process were to continue unabated, the potential would increase to the level at which Au dissolution would occur. Since Au dissolution is not desired, the galvanostatic process is set to terminate when the potential exceeds a cut-off value, V_{co}. The cut-off value is an important process parameter that must be determined for each alloy composition. In this example, the cut-off potential is set to be 1.3 V. Fig. 3b and c show that crack-free, blanket, NPG films are fabricated by this method and uniform three-dimensional porosity is obtained through the entire 250 nm thickness.

We now compare the potentiostatic and galvanostatic methods for both low Au concentration as well as high Au concentrations in the precursor alloy; the otherwise nominally identical precursor alloy films had thicknesses of 250 nm and were deposited atop an Au barrier layer, Cr adhesion layer and silicon substrate. The maximum potential in the galvanostatic method is set to be about 5% higher than the maximum potential attained in the potentiostatic method. The current density for the galvanostatic method is chosen to be 10 mA/cm^2, which is about 30% of the maximum current density observed in potentiostatic dealloying with ramped potential application. For relatively high Au composition precursor films, i.e. 32–35 at.% Au, both the potentiostatic method with ramped potential and the galvanostatic method lead to uniform crack-free NPG structures as seen in Fig. 4a and b, respectively. The total time necessary for the dealloying process to come to completion is about 5 s for the galvanostatic method and about 30 s for the potentiostatic method. This is important because, in principle, the NPG ligament and pore sizes coarsen with longer dealloying times, although the differences are not readily evident in Fig. 4. Additional experiments show that crack-free NPG films can be obtained from precursor alloy compositions larger than 32 at.% Au using the galvanostatic method for current density values between 3 mA/cm^2 and 10 mA/cm^2.

We now consider NPG films obtained from precursor alloy films with relatively low Au concentrations between 26 at.% and 30 at.% Au via both potentiostatic and galvanostatic dealloying methods. Again, the precursor films with thickness of 250 nm are deposited onto silicon substrates with the Au and Cr layers. Fig. 5a shows a NPG film obtained by step application of the potential to 1.2 V, which results in an initial Ag dissolution rate of about 1700 mA/cm^2 that drops to 25 mA/cm^2 after 1 s, then down to 10 mA/cm^2 after 2 s and finally below 1 mA/cm^2 for the next 8 s of dissolution. It is clear that the resulting NPG structure is severely cracked. The NPG structure is dramatically improved using potentiostatic dealloying with ramped potential at a rate of 1 V/min to a maximum of 1.2 V (cf. Fig. 5b). In this scheme, the maximum current density is 12 mA/cm^2 and the material removal period is around 50 s. The dramatic decrease of the maximum Ag removal rate compared to the stepped potential results in a significant improvement to structural uniformity; nonetheless, minor cracks exist with lengths varying between 50 nm and 150 nm. Fig. 5c shows the results of galvanostatic dealloying with a current density controlled to 3 mA/cm^2; the dealloying process is terminated after 62 s as the potential reached 1.26 V. For such low Au concentration precursor alloys, the galvanostatic method does not significantly reduce the density and sizes of surface damage as compared to the ramped potential scheme. The value of the constant current density is lowered even further to 1 mA/cm^2 in dealloying of an identical sample for about 200 s; Fig. 5d shows that the NPG structure has a coarser structure for lower current densities due to extended exposure time to the electrolyte and the surface damage becomes even more pronounced.

The crack-like features in Fig. 5a are comparable to the thickness of the film but they likely do not extend to the substrate because the NPG films did not delaminate. These defects probably developed during the very high current density in the first 1 s of the dealloying process. The length of the crack-like features in Fig. 5b and c is much smaller than the film thickness and can be considered to be superficial. The ligament sizes vary between 10 and 15 nm. The sizes of the crack-like features in Fig. 5d are again comparable to the film thickness. These defects likely initiated as smaller features and then grew to their present size as a consequence of coarsening of the nanostructure that occurred during the extended dealloy-

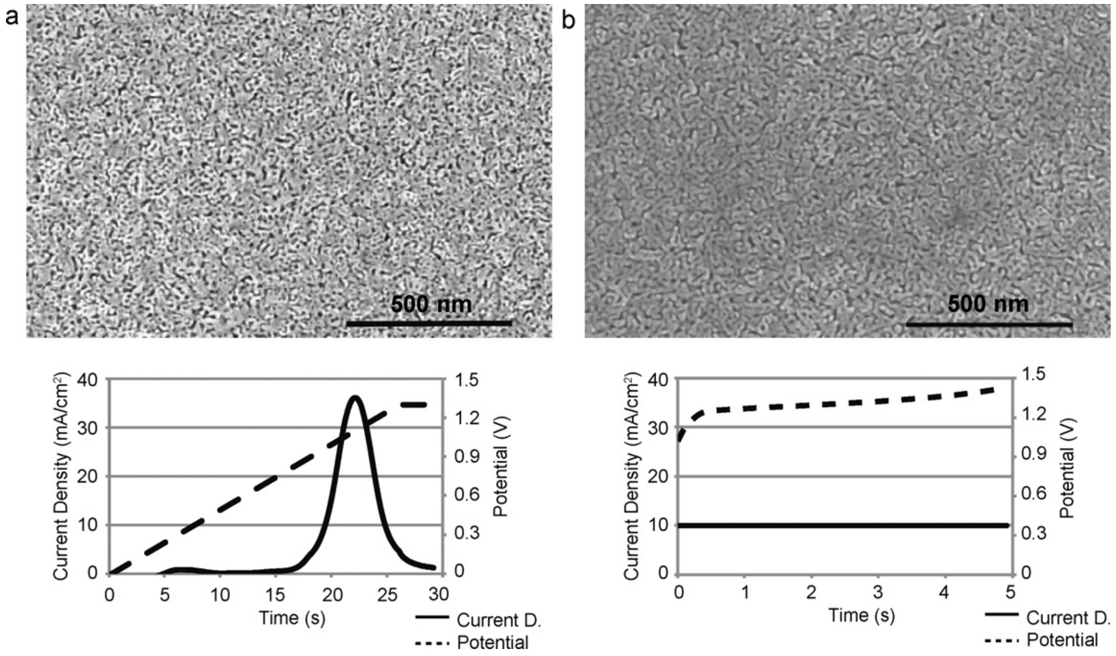

Fig. 4. Potential and current history and resulting NPG structure prepared using: (a) potentiostatic dealloying with ramped potential increase; and, (b) galvanostatic dealloying. Precursor alloy has 250 nm thickness with an initial composition of 34 at.% Au.

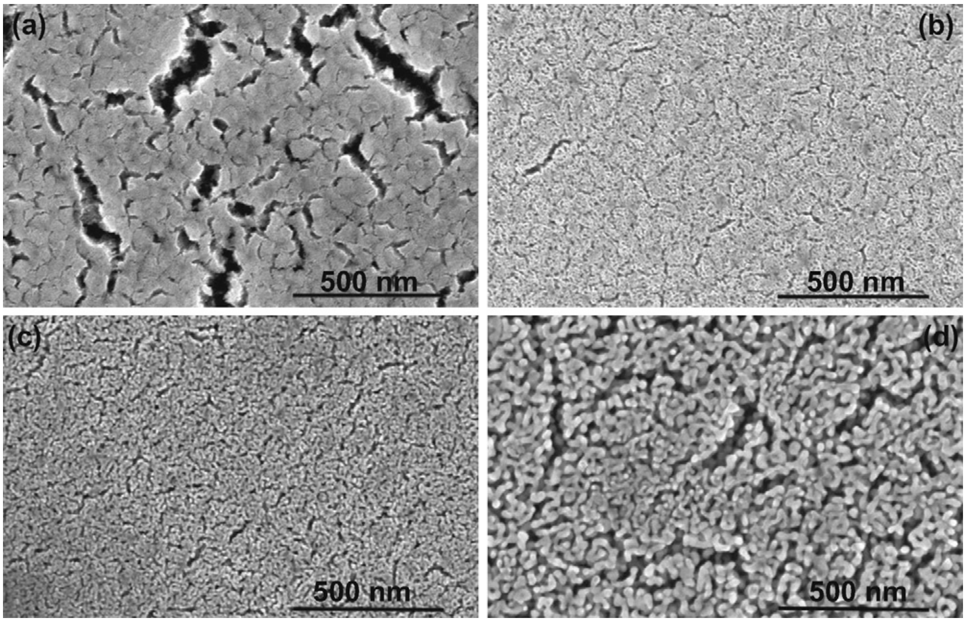

Fig. 5. NPG films from 26 at.% Au precursor alloy with 250 nm thickness fabricated by: (a) potentiostatic dealloying with step potential application (1.2 V); (b) potentiostatic dealloying with ramped potential application (1.2 V at 1 V/min); (c) galvanostatic dealloying at 3 mA/cm^2; and, (d) galvanostatic dealloying at 1 mA/cm^2.

ing period. The ligament size is about 25–30 nm due to extended exposure to the electrolyte at applied potential, i. e. electrochemical annealing. In summary, for 250 nm thick 26 at.% precursor alloy films, both the ramped potential potentiostatic scheme and the galvanostatic dealloying provide significant improvement to the NPG structure relative to the films acquired with step application of the potential. However, the final NPG film structures are in general of lower quality than those seen with a larger initial Au concentration in the precursor alloy. This observation is in agreement with the poor film quality and higher cracking tendency of the lower Au composition films reported in the literature [18,24].

Another set of experiments is carried out to compare the galvanostatic and potentiostatic dealloying methods for significantly thicker films, in this case with precursor alloy films of thickness of 1300 nm and composition of 32 at.% Au. Fig. 6a shows the results of the potentiostatic method upon the step application of a potential of 1.2 V, which yields an initial current density of about 100 mA/cm^2. It is evident that the NPG film is severely damaged with cracks that extend up to several micrometers in length, which is much larger than the film thickness. The cracks appear to initiate from the free surface of the NPG films and propagate toward the substrate. Despite severe cracking, the film does not delaminate. Occasional nanoscale cracks are observed within the islands separated by large-sized cracks. Potentiostatic dealloying was used to dealloy a nominally identical sample with ramped potential rate of 1 V/min with a maximum potential of 1.2 V that is then held constant for about 600 s until the dissolution rate decreases below 1 mA/cm^2 (cf. Fig. 6b); the peak value of Ag dissolution rate is 50 mA/cm^2. Again, large scale cracking occurred; however the width of the cracks is slightly less than for the step application of potential. Galvanostatic dealloying at a constant current density of 3 mA/cm^2 is used on a third nominally identical sample with a cut-off potential of 1.2 V. As seen in Fig. 6c, no cracks are observed over an area of many hundreds of square micrometers; however the higher magnification inset of Fig. 6c shows there to be very minor superficial damage.

The 1300 nm films have a much higher propensity for cracking than do the 250 nm thick films. The cracks observed are through-thickness channel cracks that have an in-plane length much longer than the film thickness. It is known [34] that cracks can grow in a film when the thickness exceeds a critical value given by

$$h_f^{cr} = \frac{2}{\pi c_e^2}\frac{\Gamma_f \bar{E}_f}{\sigma_m^2} \tag{1}$$

where c_e is a numerical coefficient related to the morphology of the crack, Γ_f is the energy of fracture of the thin film, $\bar{E}_f$ is the plane strain modulus of the thin film, and σ_m is the mean biaxial stress in the film due to strain mismatch of the film with respect to the substrate. Eq. (1) is strictly valid only when the elastic properties of the substrate are the same as those of the film; however the functional form of the expression is nevertheless instructive because it shows the critical thickness to decrease as the square of the stress, σ_m. The mismatch strain that leads to a non-zero σ_m is due to the mechanisms that cause shrinkage of the precursor alloy. Thus, the relationship between h_f^{cr} and σ_m is critical in terms of developing a fabrication procedure that leads to crack-free films. For the set of 1300 nm thick specimens shown in Fig. 6, both potentiostatic dealloying regimens induce a high rate of increase of σ_m as a result of high values of the current density during dealloying. On the other hand, galvanostatic dealloying at a constant current density of 3 mA/cm^2 is effective in maintaining the stress level below the critical value.

The post-dealloying compositions of the NPG films are determined by Energy Dispersive X-Ray Spectroscopy (EDS) by Princeton-Gamma Tech. Inc. using a Hitachi 4700 SEM. Due to the high thicknesses of the 1300 nm films, the underlying Si substrate and Cr adhesion layer are not detected during the analysis; thus the results are indicative of the composition of the NPG film. For the 1300 nm thick films prepared by both potentiostatic methods in Fig. 6a and b the residual Ag in the NPG films is 20 at.% Ag, whereas the NPG film prepared by galvanostatic dealloying in Fig. 6c has a residual content of 14 at.% Ag. The residual Ag concentration of the 250 nm films in this study (cf. Figs. 4 and 5) could not be measured accurately because the EDS detected the underlying Au and Cr layers. However in a previous study [18], the residual Ag concentration ranged from 2 at.% to 5 at.% Ag using the ramped potentiostatic method for 250 nm thick NPG thin films with 30 at.% to 33 at.% Au using precursor alloys that were deposited via thermal vapor deposition without an underlying Au layer. It is interesting to note that

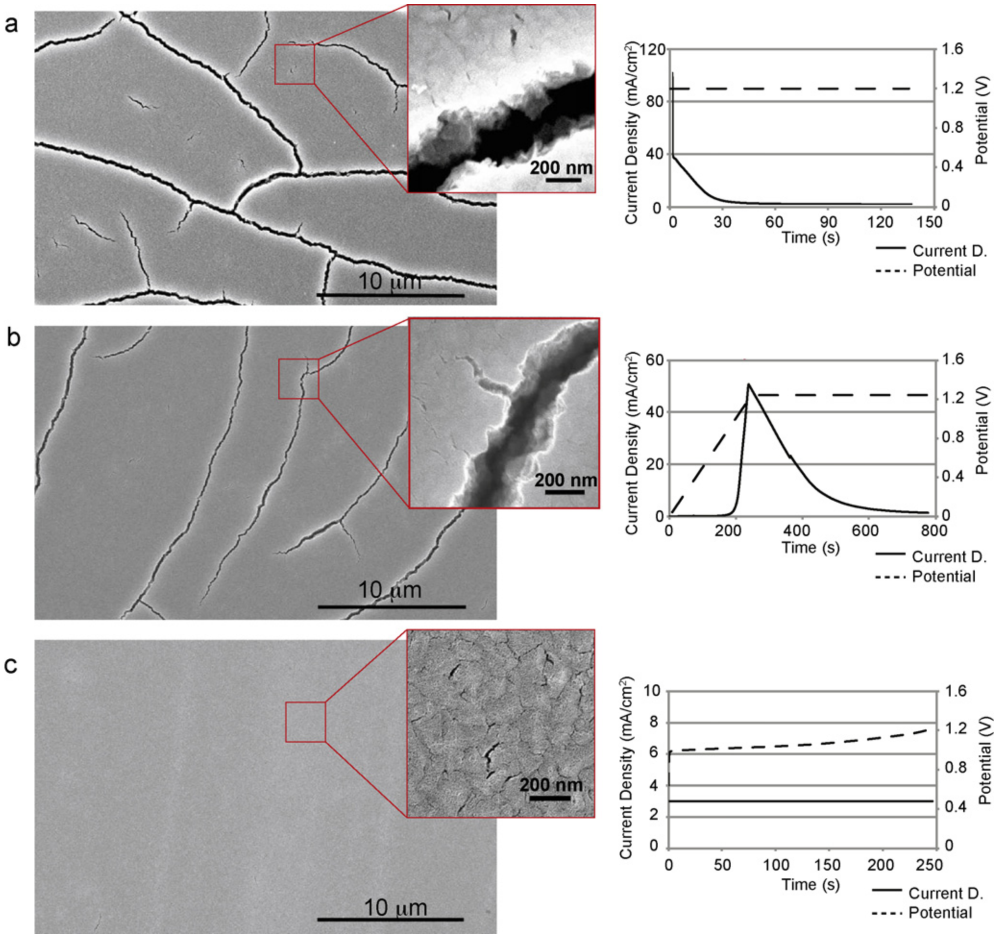

Fig. 6. Potential and current history and resulting NPG structure of 1300 nm NPG films from 32 at.% Au precursor alloy: (a) potentiostatic method with stepped potential; (b) potentiostatic method with ramped potential; and, (c) galvanostatic method with constant current density of 3 mA/cm^2.

the time necessary for complete dealloying in the cracked 1300 nm film under a ramped potential in Fig. 6b is significantly longer than the time necessary for the uncracked 250 nm films dealloyed in a ramped potential in Fig. 4a.

Surface chemistry affects the evolution of the nanoporous structure. The simple cyclic voltammetry data, acquired using a pure Au electrode as the anode, shows that around 1.26 V there is a small increase in the current reading (cf. Fig. 7). This increase corresponds to the electrosorption of a monolayer of oxygen species on the gold surface. Newman et al. [35] showed that surface mobility of the gold atoms drastically reduces in the presence of such monolayers during dealloying. The recent study by Biener et al. [36] confirms stabilization of low coordinated Au atoms by adsorbed oxygen. The electrochemical annealing is enhanced at high overpotential values, unless the potential exceeds the value at which the electrosorption occurs [37]. The oxygen species monolayer inhibits gold diffusion on the surface, so that stress relaxation is reduced. Therefore, potentiostatic dealloying performed at a potential near the onset of surface oxide formation may lead to cracking. In contrast, in galvanostatic dealloying the potential is kept below the surface oxidation threshold for the majority of the process time and it increases only due to a paucity of Ag near the end of the dealloying process. The galvanostatic method provides a more suitable dealloying regimen that results in a lower residual Ag content and yet reduces the dealloying time at potentials above the oxidation threshold, thus allowing fabrication of crack-free films with relatively large thickness.

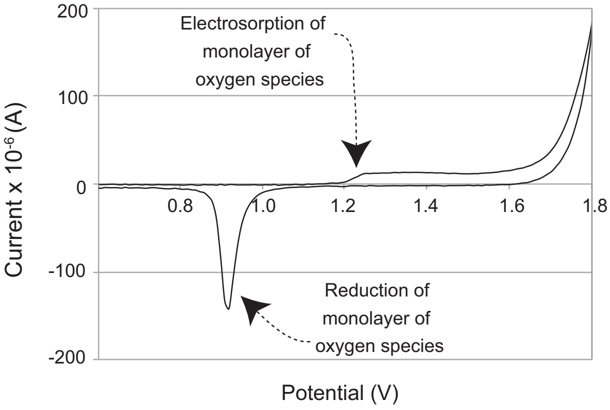

Fig. 7. Cyclic voltammetry test using Au on anode.

The ligament size in the 250 nm films is around 5–7 nm regardless of the fabrication technique. The ligament size observed in the 1300-nm-thick films is significantly smaller than those observed in 250 nm films. The underlying cause of the small feature size is not yet understood, but the film stress may play a significant role. As described by Eq. (1), the critical stress at the onset of cracking of 250-nm-thick films is more than twice that for 1300-nm-thick films, assuming the mechanical properties are the same. Therefore, the film stress achieved in the thinner films during dealloying is likely to be a factor of two larger than the film stress in the thicker films. The lower stress may affect the Ag removal and surface diffusion of Au, which would lead to smaller pores. The effect of stress on the surface construction mechanism is yet to be studied in detail.

To achieve a lower residual Ag content for the 1300 nm NPG films, a nominally identical sample is dealloyed using galvanostatic dealloying at a lower current density of 1.5 mA/cm^2 and a higher cut-off potential of 1.45 V; both changes serve to increase the total time of dealloying. The potential and current density histories are shown in Fig. 8a. Fig. 8b shows the surface of the resulting NPG film and Fig. 8c shows the cross-section, which demonstrates that the uniform porous structure observed on the surface of the film is preserved through the thickness of the films. The EDS measurements show the residual silver content to be 1.5 at.% Ag. It is also evident in comparing the insets of Figs. 6c and 8c that the ligament and pore sizes of the NPG films are significantly larger when dealloyed at the lower current density and higher cut-off potential; in addition there is no superficial surface damage in the film shown in Fig. 8c. The high residual Ag content together with the small pore sizes observed in thick films in Fig. 6c suggests mass transport through the pores of the thick film may play the limiting role in the removal of Ag.

We now demonstrate that the current readings acquired during dealloying represent the Ag dissolution. To this end, cyclic voltammetry tests are performed to observe the oxidation peaks on a 99.999% pure Au (Alfa Aesar) wire electrode (cf. Fig. 7). The current versus potential curve in Fig. 7 shows that—for the electrolyte used in this study—a monolayer of surface oxide forms on the surface at around 1.26 V, so for cut-off potentials above this value a surface oxide monolayer can be assumed to exist on the final NPG surface. In addition, in this electrolyte, the oxidation of water as described in

$$2H_2O \rightarrow O_2(g) + 2H^+(l) + 2e^- \qquad (2)$$

takes place at a value greater than 1.6 V and the dissolution of Au occurs at an even higher potential. Thus, for the potential values used in this study for both galvanostatic and potentiostatic dealloying methods, the current density represents the dissolution of only Ag, except for the very minor contribution to the current density due to the formation of the surface oxide monolayer.

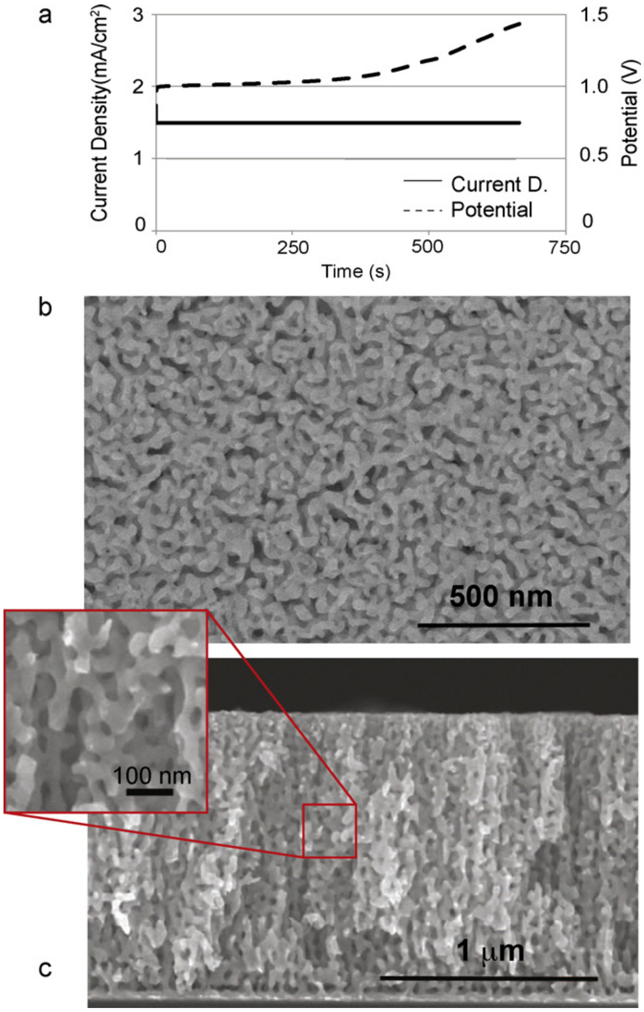

Fig. 8. Galvanostatic dealloying of a 1300 nm thick precursor of 32 at.% Au to achieve a crack-free NPG film with lower residual Ag content: (a) potential history for 1.5 mA/cm^2 current density; (b) surface of crack-free blanket NPG film; and, (c) cross-sectional view.

5. Conclusions

The fabrication of crack-free NPG thin films constrained to a rigid substrate poses significant difficulties due to the dimensional constraints of the substrate and the resulting stress field. If NPG thin films are to be incorporated into micro-electro-mechanical (MEMS) devices, essential requirements of a fabrication method include:

- no cracks,
- 3-dimensional porosity, and
- surface uniformity.

An ideal fabrication method for such films should be versatile and provide the flexibility to tailor the film properties over a wide range. Thus, the method should enable fabrication of films with:

- minimum residual Ag,
- tailorable ligament size,
- and minimum processing time (to minimize fabrication cost).

Existing potentiostatic methods provide effective fabrication techniques; however, they have drawbacks which include multistep dealloying processes as well as dealloying times that range from several hours up to 70 h for bulk materials [15,23] or from 10 min to 35 min for 75 nm thin films [16]. Clearly the current densities over such extended times remain very low, which allow crack-free NPG to be obtained. However, the small electric potential that must be applied in order to achieve such low current densities may leave a relatively large residual Ag concentration in the NPG [23]. On the other hand, with the galvanostatic methods we introduce, the dealloying times range from a few seconds to a few minutes, depending upon the thickness and initial composition of the precursor film. In addition, since the galvanostatic method must vary the potential to maintain a constant areal current density, the potential near the end of the dealloying processes achieves a sufficiently high value to allow a low residual Ag concentration.

The mechanisms of change of film stress with Ag removal rate is not yet well understood. The Ag removal rate is temporally highly non-uniform for high potential values using potentiostatic methods, so that stress increase rates are also very high, which may enhance cracking. However, potentiostatic dealloying at low potentials [23], or in multiple steps [15], has been shown to decrease the volume shrinkage in unconstrained films.

We show that the most effective way to achieve crack-free films with low residual Ag content is to control directly the dissolution rate of the Ag in an electrochemical cell. Potentiostatic methods for which the potential is increased either as a step or as a ramp function do not allow full control of the Ag dissolution rate because the current density—which is directly related to the dissolution rate of Ag—is a function of the applied potential and the details of the electrochemical circuit. However galvanostatic dealloying—which directly controls the current density and hence the Ag dissolution rate—in an electrochemical cell is shown to be superior to the potentiostatic dealloying method with regard to obtaining blanket crack-free NPG thin films. As opposed to the potentiostatic method, in the galvanostatic method the current density is controlled and the electrical potential is a function of the prescribed current and the details of the electrochemical circuit.

For 250 nm thick precursor alloy films with a relatively high Au concentration in the range of 32–35 at.% Au, a galvanostatic method as well as a ramped application of potential in a potentiostat yields crack-free NPG thin films. However for a lower Au concentration of 26–30 at.% Au, while both methods yield NPG films that are free of major cracks, there is some minor superficial damage.

For 1300 nm thick precursor alloy films, the galvanostatic method allows the fabrication of crack-free NPG films with negligible superficial damage from precursor alloys with 32 at.% Au concentration. Potentiostatic dealloying using both a step as well as a ramp potential application is not able to achieve crack-free NPG films of this thickness. The precise control of the Ag dissolution rated enabled by galvanostatic dealloying is the key to maintaining the stress below the critical value at which extensive cracking is observed.

For both potentiostatic and galvanostatic dealloying methods, there is no systematic variation in pore and ligament size through the thickness. However superficial damage and small-scale cracks are observed on most films at lower Au concentrations in the precursor alloy. Crack-free films as thick as 1300 nm with only minor superficial damage are obtained using the galvanostatic method from a 32 at.% precursor alloy. Thus the final film quality and surface morphology strongly depend on the initial alloy composition.

In summary, galvanostatic dealloying is effective in the fabrication of crack-free blanket NPG films with a residual of 1.5 at.% Ag up to a thickness of 1300 nm over many hundreds of square micrometers. The method should prove to be useful in the fabrication of micro-electro-mechanical system (MEMS) devices with NPG coatings of high quality.

Acknowledgments

Support from NSF CMMI-0826093 is gratefully acknowledged. In addition, this research was carried out in part at the Center for Functional Nanomaterials, Brookhaven National Laboratory, which is supported by the U.S. Department of Energy, Office of Basic Energy Sciences, under Contract No. DE-AC02-98CH10886. The authors thank U. Emekli, J. Wu and A.C. West for enlightening discussions, and A. Steege for assistance with the experimental set-up.

References

[1] J. Snyder, K. Livi, J. Erlebacher, Journal of the Electrochemical Society 155 (8) (2008) C464–C473.
[2] J. Weissmüller, R.C. Newman, H.J. Jin, A.M. Hodge, J.W. Kysar, MRS Bulletin 34 (8) (2009) 577–586.
[3] R. Zeis, A. Mathur, G. Fritz, J. Lee, J. Erlebacher, Journal of Power Sources 165 (1) (2007) 65–72.
[4] H.-J. Jin, S. Parida, D. Kramer, J. Weissmueller, Surface Science 602 (23) (2008) 3588–3594.
[5] D. Kramer, R.N. Viswanath, J. Weissmüller, Nano Letters 4 (5) (2004) 793–796.
[6] J. Weissmüller, R. Viswanath, D. Kramer, P. Zimmer, R. Wurschum, H. Gleiter, Science 300 (5617) (2003) 312–315.
[7] M.M. Biener, J. Biener, C.M. Friend, Langmuir 21 (5) (2005) 1668–1671.
[8] J. Biener, A. Wittstock, L.A. Zepeda-Ruiz, M.M. Biener, V. Zielasek, D. Kramer, R.N. Viswanath, J. Weissmüller, M. Baeumer, A.V. Hamza, Nature Materials 8 (1) (2009) 47–51.
[9] R. Zeis, T. Lei, K. Sieradzki, J. Snyder, J. Erlebacher, Journal of Catalysis 253 (1) (2008) 132–138.
[10] A. Wittstock, V. Zielasek, J. Biener, C.M. Friend, M. Baumer, Science 327 (5963) (2010) 319–322.
[11] E. Seker, Y. Berdichevsky, M.R. Begley, M.L. Reed, K.J. Staley, M.L. Yarmush, Nanotechnology 21 (12) (2010) 125504.
[12] Y. Ding, M. Chen, MRS Bulletin 34 (8) (2009) 569–576.
[13] S.O. Kucheyev, J.R. Hayes, J. Biener, T. Huser, C.E. Talley, A.V. Hamza, Applied Physics Letters 89 (5) (2006) 053102.
[14] M.C. Dixon, T.A. Daniel, M. Hieda, D.M. Smilgies, M.H.V. Chan, D.L. Allara, Langmuir 23 (5) (2007) 2414–2422.
[15] Y. Sun, T.J. Balk, Scripta Materialia 58 (9) (2008) 727–730.
[16] Y. Sun, K.P. Kucera, S.A. Burger, T.J. Balk, Scripta Materialia 58 (11) (2008) 1018–1021.
[17] M. Kim, W.J. Ha, J.W. Anh, H.S. Kim, S.W. Park, D. Lee, Journal of Alloys and Compounds 484 (1–2) (2009) 28–32.
[18] O. Okman, D. Lee, J.W. Kysar, Scripta Materialia 63 (10) (2010) 1005–1008.
[19] A.J. Forty, Nature 282 (5739) (1979) 597–598.
[20] H.W. Pickering, Corrosion Science 23 (10) (1983) 1107–1109, 1111–1120.
[21] A. Mathur, J. Erlebacher, Applied Physics Letters 90 (6) (2007) 061910.
[22] C.A. Volkert, E.T. Lilleodden, D. Kramer, J. Weissmüller, Applied Physics Letters 89 (6) (2006) 061920.
[23] S. Parida, D. Kramer, C.A. Volkert, H. Rösner, J. Erlebacher, J. Weissmüller, Physical Review Letters 97 (3) (2006) 035504.
[24] N.A. Senior, R.C. Newman, Nanotechnology 17 (9) (2006) 2311–2316.
[25] J. Rösler, O. Näth, S. Jäger, F. Schmitz, D. Mukherji, Acta Materialia 53 (5) (2005) 1397–1406.
[26] E. Seker, J.T. Gaskins, H. Bart-Smith, J. Zhu, M.L. Reed, G. Zangari, R. Kelly, M.R. Begley, Acta Materialia 55 (14) (2007) 4593–4602.
[27] D.A. Crowson, D. Farkas, S.G. Corcoran, Scripta Materialia 61 (5) (2009) 497–499.
[28] J. Weissmüller, H.L. Duan, D. Farkas, Acta Materialia 58 (1) (2010) 1–13.
[29] J. Erlebacher, M.J. Aziz, A. Karma, N. Dimitrov, K. Sieradzki, Nature 410 (6827) (2001) 450–453.
[30] R. Li, K. Sieradzki, Physical Review Letters 68 (8) (1992) 1168–1171.
[31] J. Biener, A.M. Hodge, A.V. Hamza, Applied Physics Letters 87 (12) (2005) 121908.
[32] D. Lee, X. Wei, X. Chen, M. Zhao, S.C. Jun, J. Hone, E.G. Herbert, W.C. Oliver, J.W. Kysar, Scripta Materialia 56 (5) (2007) 437–440.
[33] J. Erlebacher, K. Sieradzki, Scripta Materialia 49 (10) (2003) 991–996.
[34] L.B. Freund, S. Suresh, Thin Film Materials: Stress, Defect Formation, and Surface Evolution, Cambridge University Press, Cambridge, UK, 2003.
[35] R.C. Newman, S.G. Corcoran, J. Erlebacher, M.J. Aziz, K. Sieradzki, MRS Bulletin 24 (7) (1999) 24–28.
[36] J. Biener, M.M. Biener, T. Nowitzki, A.V. Hamza, C.M. Friend, V. Zielasek, M. Baeumer, Chemphyschem 7 (9) (2006) 1906–1908.
[37] J. Biener, A. Wittstock, M.M. Biener, T. Nowitzki, A.V. Hamza, M. Baeumer, Langmuir 26 (17) (2010) 13736–13740.